ORIGINAL ARTICLE

Cancer Science WILEY

PP6 deficiency in mice with KRAS mutation and Trp53 loss promotes early death by PDAC with cachexia-like features

Katsuya Fukui[1,2,3] | Miyuki Nomura[1] | Kazuhiro Kishimoto[1,2,4] | Nobuhiro Tanuma[1,2] |
Koreyuki Kurosawa[1,2,5] | Kosuke Kanazawa[1,2,6] | Hiroyuki Kato[1] | Tomoki Sato[7] |
Shinji Miura[7] | Koh Miura[1,6] | Ikuro Sato[8] | Hiroyuki Tsuji[4] | Yoji Yamashita[1] |
Keiichi Tamai[9] | Toshio Watanabe[10] | Jun Yasuda[2,11] | Takuji Tanaka[12] |
Kennichi Satoh[13] | Toru Furukawa[14] | Keiichi Jingu[3] | Hiroshi Shima[1,2]

[1]Division of Cancer Chemotherapy, Miyagi Cancer Center Research Institute, Natori, Japan

[2]Division of Cancer Molecular Biology, Tohoku University Graduate School of Medicine, Sendai, Japan

[3]Department of Radiation Oncology, Tohoku University Graduate School of Medicine, Sendai, Japan

[4]Department of Head and Neck Surgery, Kanazawa Medical University, Kanazawa, Japan

[5]Department of Plastic and Reconstructive Surgery, Tohoku University Graduate School of Medicine, Sendai, Japan

[6]Division of Surgery, Miyagi Cancer Center, Natori, Japan

[7]Laboratory of Nutritional Biochemistry, Graduate School of Nutritional and Environmental Sciences, University of Shizuoka, Shizuoka, Japan

[8]Division of Pathology, Miyagi Cancer Center, Natori, Japan

[9]Division of Cancer Stem Cell, Miyagi Cancer Center Research Institute, Natori, Japan

[10]Department of Biological Science, Graduate School of Humanities and Sciences, Nara Women's University, Nara, Japan

[11]Division of Molecular Cellular Oncology, Miyagi Cancer Center Research Institute, Natori, Japan

[12]Research Center of Diagnostic Pathology, Gifu Municipal Hospital, Gifu, Japan

[13]Division of Gastroenterology, Tohoku Medical Pharmaceutical University, Sendai, Japan

[14]Department of Investigative Pathology, Tohoku University Graduate School of Medicine, Sendai, Japan

Correspondence
Hiroshi Shima, Division of Cancer Chemotherapy, Miyagi Cancer Center Research Institute, 47-1 Nodayama, Medeshima-Shiode, Natori, Miyagi 981-1293, Japan.
Email: shima@med.tohoku.ac.jp

Abstract

To examine effects of PP6 gene (*Ppp6c*) deficiency on pancreatic tumor development, we developed pancreas-specific, tamoxifen-inducible Cre-mediated KP (KRAS(G12D) plus Trp53-deficient) mice (cKP mice) and crossed them with *Ppp6c^{flox/flox}* mice. cKP mice with the homozygous *Ppp6c* deletion developed pancreatic tumors, became emaciated and required euthanasia within 150 days of mutation induction, phenotypes that were not seen in heterozygous or wild-type (WT) mice. At 30 days, a comparative analysis of genes commonly altered in homozygous versus WT *Ppp6c* cKP mice revealed enhanced activation of Erk and NFκB pathways in homozygotes. By 80 days, the number and size of tumors and number of precancerous lesions had significantly increased in the pancreas of *Ppp6c* homozygous relative to heterozygous or WT cKP mice. *Ppp6c^{−/−}* tumors were pathologically diagnosed as pancreatic

Katsuya Fukui, Miyuki Nomura, and Kazuhiro Kishimoto are contributed equally to this work.

ductal adenocarcinoma (PDAC) undergoing the epithelial–mesenchymal transition (EMT), and cancer cells had invaded surrounding tissues in three out of six cases. Transcriptome and metabolome analyses indicated an enhanced cancer-specific glycolytic metabolism in *Ppp6c*-deficient cKP mice and the increased expression of inflammatory cytokines. Individual $Ppp6c^{-/-}$ cKP mice showed weight loss, decreased skeletal muscle and adipose tissue, and increased circulating tumor necrosis factor (TNF)-α and IL-6 levels, suggestive of systemic inflammation. Overall, *Ppp6c* deficiency in the presence of *K-ras* mutations and *Trp53* gene deficiency promoted pancreatic tumorigenesis with generalized cachexia and early death. This study provided the first evidence that *Ppp6c* suppresses mouse pancreatic carcinogenesis and supports the use of *Ppp6c*-deficient cKP mice as a model for developing treatments for cachexia associated with pancreatic cancer.

KEYWORDS
cachexia, IL-6, *K-ras*, pancreatic ductal adenocarcinoma, protein phosphatase 6

1 | INTRODUCTION

Pancreatic ductal adenocarcinoma (PDAC) is an extremely deadly cancer, with a 5-year survival rate of only 10%.[1] Genetic alterations such as activating mutations in *K-ras* or *TGF-β* and inactivation of tumor suppressors such as *p53*, *INK4A/ARF*, *BRCA2* and *Smad4* are the most common drivers of pancreatic carcinogenesis.[2,3] Despite critical advances in our understanding of the molecular basis of this cancer, pancreatic cancer chemotherapy is still inadequate in terms of the range of drugs available and their efficacy, and development of new therapies is still required.[4]

More than 30% of all human cancers, including 95% of pancreatic cancers, are driven by mutations in the RAS family genes.[5] However, clinically, mutant RAS remains an elusive target despite substantial investigation of the strategies to attack mutant RAS.[5] Interestingly, a recent large-scale ethyl methanesulfonate (EMS) genetic screen in *Drosophila* identified the loss of the protein phosphatase 6 (PP6) gene (*Ppp6c*) as cooperating with oncogenic RAS to induce tumor cell proliferation and invasion, suggesting that *Ppp6c* serves as a tumor suppressor in RAS-related cancers.[6] We also showed that *Ppp6c* deficiency in a mouse model of *K-ras*-mutant intraepithelial carcinoma increased the incidence of tumors of the tongue at ~2 weeks after induction of *Ppp6c* deficiency,[7] supporting a PP6 tumor suppressor function in this context. However, in our analysis, mice died of malnutrition as enlarged tongue tumors interfered with feeding,[7] and *Ppp6c* involvement in malignant transformation of those tumors remains unclear.

PP6 associates with a regulatory subunits (PP6R1, PP6R2, or PP6R3) and a scaffold subunits (ANKRD28, ANKRD44, or ANKRD52), which together form a heterotrimer.[8] The diversity of these subunits allows PP6 to regulate a wide range of biological processes, including cell cycle progression, the DNA damage response, miRNA processing, and the regulation of cell/tissue volume.[8] PP6 also reportedly regulates NFκB signaling[9] by blocking IkBε degradation in response to TNF-α[10] and inactivation of TAK1 in the IL-1 signaling pathway.[11] A recent shRNA screen identified PP6 as a phosphatase that dephosphorylates MEK.[12] Pathologically, analysis of tissues from cancer patients supports the idea that *Ppp6c* functions as a tumor suppressor. *Ppp6c* is reportedly mutated in 9% of human melanoma specimens[13] and 15% of human skin basal cell carcinoma tissues,[14] suggestive of a tumor suppressor function in skin tumors. In agreement with these findings, we conducted carcinogenesis experiments in mice and found that *Ppp6c* deficiency increased tumorigenesis in UV-induced BRAF(V600E)-initiated melanomagenesis,[15] and UV-induced skin squamous cell carcinogenesis.[16]

The Cancer Genome Atlas (TCGA) database showed that 70% of cases with mutations in *K-ras* in PDAC also have truncating or missense mutations in *p53*. Therefore, here we asked whether *Ppp6c* functioned as a tumor suppressor gene in pancreatic cancer in the context of KRAS(G12D) mutations and *Trp53* deficiency. To do so, we generated tamoxifen (TAM)-induced, Cre-mediated KP (KRAS(G12D) +Trp53 deficient) (cKP) mice and then crossed them with $Ppp6c^{flox/flox}$ mice[17] to determine whether *Ppp6c* deficiency promotes pancreatic carcinogenesis in the cKP model.

2 | MATERIALS AND METHODS

2.1 | Generation of mice with inducible K-ras^{G12D} expression, Trp53 deletion, and Ppp6c deletion in pancreas

$Pdx1\text{-}CreER^{T2}/K\text{-}ras^{LSL-G12D/+}/Trp53^{flox/flox}/Ppp6c^{+/+}$ (designated cKP(+/+) mice), $Pdx1\text{-}CreER^{T2}/K\text{-}ras^{LSL-G12D/+}/Trp53^{flox/flox}/Ppp6c^{flox/+}$ (designated cKP(F/+) mice), and $Pdx1\text{-}CreER^{T2}/K\text{-}ras^{LSL-G12D/+}/Trp53^{flox/flox}/Ppp6c^{flox/flox}$ (designated cKP(F/F) mice) were generated as described in Doc S1. All animal experiments were performed with approval of the Miyagi Cancer Center Research Institute Animal Care and Use committee (MCCAE-2020-1 and AE.21.10).

2.2 | TAM administration

To induce recombination of floxed alleles in pancreas, TAM was administered through mother's milk to all mice for 7 days from starting at postnatal day 0 through day 6. To do so, TAM (1.5 mg; Sigma-Aldrich) was administered to lactating females via daily intraperitoneal injection for 7 days.

2.3 | PCR genotype analysis

Recombined genes were confirmed by PCR, as previously described.[7,17] Details are provided in Doc S1.

2.4 | Western blot analysis

Western blot analysis was done as previously described.[18] Details are provided in Doc S1.

2.5 | Histopathology and immunohistochemistry

Histopathology and immunohistochemistry were performed as previously described.[19] Antibodies used are listed in Doc S1. Three pathologists (TF, IS, and TT) made differential pathological diagnoses.

2.6 | Quantitative real-time PCR (qRT-PCR)

qRT-PCR analyses were performed as described previously.[17] Primers and TaqMan probes newly used are provided in Doc S1.

2.7 | Serum tests

Albumin, free fatty acids, glycerol, and cytokines including IL-6, TNF-α, IL-1β, and Ccl2 in sera were analyzed as described in Doc S1.

2.8 | Transcriptome analysis

RNA extraction and sequencing, and evaluation of levels of differentially expressed genes between groups, was performed as previously described.[7] For details, please refer to Doc S1.

2.9 | Metabolomic analysis

Metabolome measurements were carried out through a facility service at Human Metabolome Technologies, Inc., as described previously.[20] For more information, please refer to Doc S1.

2.10 | Statistical analysis

Kaplan–Meier survival curves and corresponding statistical analysis, as well as log-rank tests, were done using Prism version 8 (GraphPad Software Inc.). Other statistical analyses were performed using Student's t test or the Mann–Whitney U test. A p-value of $p < 0.05$ was considered significant. Data are presented as means with SEM. $^*p < 0.05$, $^{**}p < 0.01$, $^{***}p < 0.001$, $^{****}p < 0.0001$.

3 | RESULTS

3.1 | Ppp6c loss leads to early death from cancer in mice with KRAS(G12D) and Trp53-deficient pancreatic cells

Starting with pancreas-specific, TAM-dependent CreER^{T2} inducible KRAS(G12D) plus *Trp53*-deficient mice (cKP mice: *Pdx1-CreER^{T2}/K-ras$^{LSL-G12D/+}$/Trp53 $^{flox/flox}$*), we generated three additional lines: mice homozygous for the *Ppp6c* floxed allele (*Ppp6c$^{flox/flox}$*), mice heterozygous for that allele (*Ppp6c$^{flox/+}$*), and *Ppp6c* WT (*Ppp6c$^{+/+}$*) mice. We designate these lines cKP(F/F), cKP(F/+) and cKP(+/+), respectively (Figure 1Aa). Mice were administered TAM derived from mothers' milk starting immediately after birth and continuing for 7 days. At 20 days of age, mice were sacrificed and pancreatic tissues were assessed for genomic recombination. In cKP(+/+), cKP(F/+) and cKP(F/F) mice, we observed recombination of the *K-ras$^{LSL-G12D}$* (Figure 1Ab), and *Trp53^{flox}* (Figure 1Ac), and *Ppp6c^{flox}* (Figure 1Ad) alleles.

Using different groups of mice, we administered TAM following the same protocol to cKP(+/+) ($n = 9$), cKP(F/+) ($n = 14$) and cKP(F/F) ($n = 18$) mice, then monitored for tumor development and mortality. Mice that became debilitated or showed impaired mobility were euthanized in accordance with animal ethics regulations. cKP(F/F) mice began to die at 50 days, 90% died by 100 days and all had died by 150 days, and at euthanasia all mice exhibited pancreas tumors (data not shown). By contrast, most cKP(F/+) and (+/+) mice survived up to 150 days, but ~25% of both groups became weak and died by 200 days (Figure 1B). All of these mice exhibited pancreatic tumors (data not shown). These findings indicated that *Ppp6c* deficiency accelerates the death of cKP mice.

3.2 | Ppp6c deficiency activates Erk and NFκB signaling in pancreas tissue of cKP mice

To investigate factors underlying early carcinogenesis, we analyzed signaling pathways potentially altered at early stages in pancreatic tissues of TAM-treated, *Ppp6c*-deficient cKP mice at 30 days of age. To analyze the effect of *Ppp6c* defect on RAS downstream, we examined phosphorylation of Erk and Akt, major RAS effectors.[5] To analyze the effect of *Ppp6c* defect on NFκB
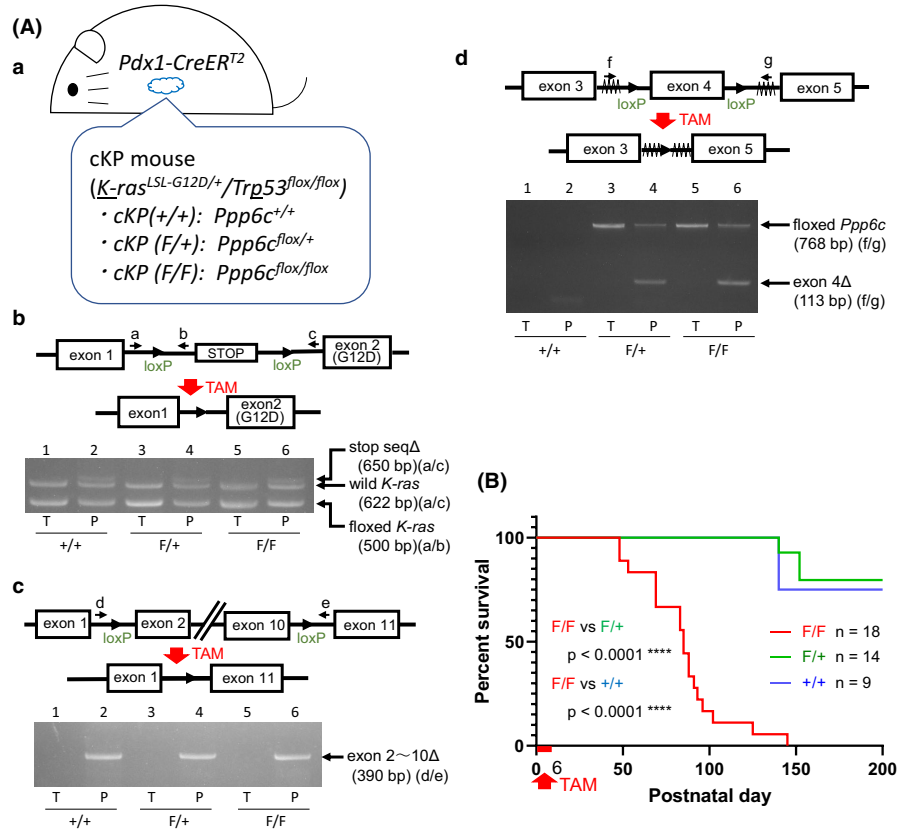
FIGURE 1 *Ppp6c* deficiency promotes the early death of cKP mice. (A) Genotypes of cKP mice and CreER[T2]-mediated gene recombination. (a) Genotypes of cKP mice. cKP(+/+), cKP(F/+), and cKP(F/F) symbols denote respective genotypes *Pdx1-CreER[T2]/K-ras[LSL–G12D/+]/Trp53[flox/flox]/Ppp6c^{+/+}*, *Pdx1-CreER[T2]/K-ras[LSL–G12D/+]/Trp53[flox/flox]/Ppp6c[flox/+]*, and *Pdx1-CreER[T2]/K-ras[LSL–G12D/+]/Trp53[flox/flox]/Ppp6c[flox/flox]*. (b) CreER[T2]-mediated *Kras[G12D]* expression. (top) Schematic representation of a *K-ras[LSL–G12D]* allele and deletion of the transcription stop sequence by activated CreER[T2]. Positions of primers a, b, and c are indicated. (bottom) PCR analysis of recombined allele. Lanes 1 and 2: cKP(+/+) mice, lanes 3 and 4: cKP(F/+) mice, and lanes 5 and 6 cKP(F/F) mice. Lanes 2, 4 and 6: genomic DNA from the pancreas of mice fed milk from TAM-injected mothers at 20 days of age (P). Lanes 1, 3 and 5: genomic DNA from tail of corresponding mice (T). Fragments of 650, 622 and 500 bp correspond to the stop sequence-deleted allele, wild-type allele, and floxed alleles, respectively. (c) CreER[T2]-mediated *Trp53* disruption. (top) Schematic showing *p53*-floxed allele and deletion of exons 2–10 by activated CreER[T2]. Positions of primers d and e are indicated. (lower) PCR analysis of recombined allele. Lanes 1–6 are as indicated in (b). A fragment of 390 bp corresponds to the deleted allele. (d) CreER[T2]-mediated *Ppp6c* disruption. (top) Schematic of *Ppp6c*-floxed and deletion of exon 4 following CreER[T2] activation. Positions of primers f and g are indicated. Serrated regions, vector sequence. (bottom) PCR analysis of recombined allele. Lanes 1–6 are as indicated in (b). Fragments of 768 bp and 113 bp length correspond to floxed and exon 4-deleted alleles, respectively. (B) *Ppp6c* deficiency promotes the early death of cKP mice. cKP(+/+) (n = 9), cKP(F/+) (n = 14) and cKP(F/F) (n = 18) mice were used for this experiment. Newborns were administered TAM via mothers' milk from days 0 to 6. On becoming debilitated, mice were euthanized in accordance with ethical guidelines for animal experimentation

signaling, we examined phosphorylation of the RelA subunit of NFκB.[21] Immunoblot analysis showed that, compared with effects seen in +/+ and F/+ mice, phosphorylation of Erk and RelA was markedly elevated in the cKP(F/F) pancreas (Figure 2A, lane 3), but there was no significant difference in Akt phosphorylation (Figure 2A, lane 3).

Next, we used histological analysis to determine which cells showed Erk and RelA activation (Figure 2B). H&E staining analysis revealed a greater number of acinar-to-ductal metaplasia (ADM) lesions in the pancreas of F/F (Figure 2Bb) compared with F/+ (Figure 2Ba) or +/+ mice (data not shown).

Analysis using immunohistochemistry (IHC) showed strong staining for phosphorylated Erk1/2 primarily in ADM lesions

and moderately strong staining in dedifferentiated acinal cells in the cKP(F/F) pancreas (Figure 2Bd), while staining was weak in cKP(F/+) (Figure 2Bc) or cKP(+/+) (data not shown) mice. IHC with RelA antibody showed strong RelA stainability mainly in ADM lesions and moderately strong stainability in dedifferentiated acinar cells of the cKP(F/F) pancreas (Figure 2Bf), and some of that staining was found in the nucleus (please refer to inset of Figure 2Bf). RelA staining was weak in cKP(F/+) (Figure 2Be) and cKP(+/+) (data not shown) mice. These data suggested that Erk and RelA activation was enhanced with the emergence of ADM in cKP(F/F) mice.

We next investigated the effects of *Ppp6c* deletion on gene expression in three sets of pancreas tissues from *Ppp6c* (F/F) and (F/+) mice. The heatmap shown in Figure 2C represents gene expression
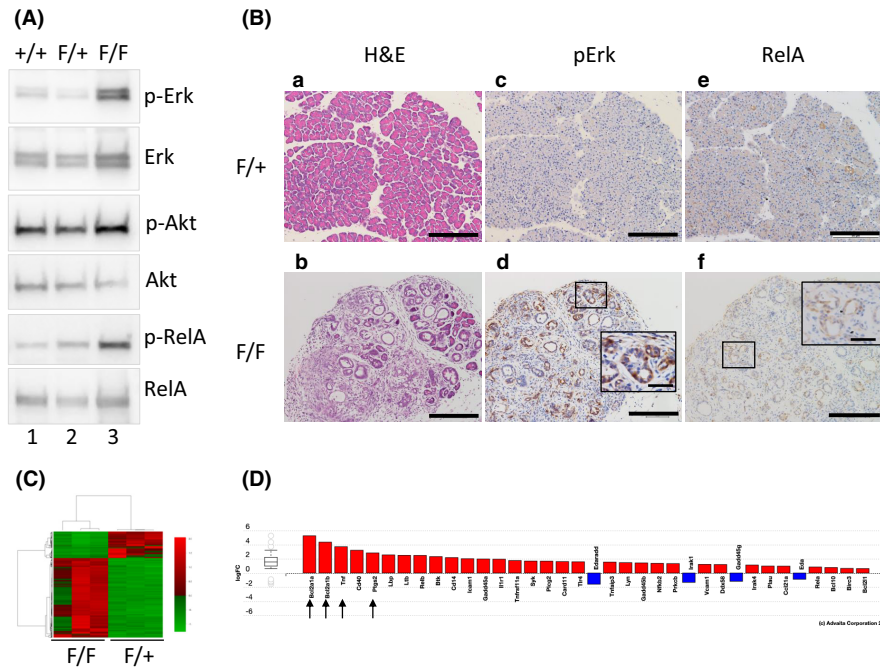
FIGURE 2 *Ppp6c* deletion in cKP mice promotes development of precancerous lesions with enhanced Erk and NFκB signaling by 30 days of age. TAM was administered to three cKP(+/+), 3 cKP(F/+), and three cKP(F/F) mice as shown in Figure 1B, and pancreatic tissues were examined at 30 days of age. (A) *Ppp6c* deficiency promotes phosphorylation of Erk and RelA/p65. Immunoblot of pancreas samples using anti-phospho Erk, anti-Erk, anti-phospho Akt, anti-Akt, anti-phospho RelA, anti-RelA antibodies. Representative data from three independent experiments are shown. Line 1: cKP(+/+), Line 2: cKP(F/+), and line 3: cKP(F/F). (B) Microscopic view of pancreas from cKP(F/F) and (F/+) mice. Shown is representative H&E staining plus immunohistochemistry with anti-phospho Erk and anti-RelA antibodies. Scale bar: 200 μm. Insets in (d) and (f) represent higher magnification images of corresponding boxed areas. Scale bar in inset: 50 μm. (C) Heatmap showing gene expression in pancreas of cKP(F/F) (n = 3) and (F/+) (n = 3) mice. Pancreatic tissues were harvested for mRNA preparation and transcriptomic analysis. The heatmap was generated as described in Section 2. In total, 17,640 genes expressed in at least one group in each comparison were used for analysis. Red and green colors indicate high and low expression levels, respectively. (D) Expression of genes functioning in NFκB signaling (KEGG 4064) in cKP(F/F) relative to (F/+) pancreas. mRNA was extracted from pancreas tissues and RNA-seq performed as in described in Section 2. The figure was generated using iPathwayGuide (Advaita Bioinformatics) software. Log FC: log of fold-change in gene expression. Box and whisker plot: box ends are upper and lower quartiles, and the span represents the interquartile range. Horizontal line inside box is the median, and whiskers indicate highest and lowest observations. Intensity levels correspond to the extent of upregulation (red) or downregulation (blue) of genes differentially expressed in cKP(F/F) versus cKP(F/+) pancreas. Arrows indicate RelA/p65 targets

in pancreatic tissue from cKP(F/F) and cKP(F/+) genotypes and indicates that expression patterns differed significantly between *Ppp6c*-deficient and -heterozygous mice. Table 1 shows ratios of gene expression in F/F relative to F/+ seen at both 30 and 80 days. Relevant to Erk signaling, expression of *Fos* and *EGR-1*, major effectors of Erk,[22] increased in cKP(F/F) pancreas (Table 1A, 30 days). Upregulation of Erk signaling was supported by our observation of increased levels of the phosphatases DUSP4, 5, 6, and 10, whose expression increased as a result of negative feedback[22] (Table 1A, 30 days). As shown in Figure 2D expression of 36 genes associated with NFκB signaling[21] either increased or decreased in a statistically significant manner (q < 0.05) at 30 days. Importantly, *Bcl2a1a* and *Bcl2a1b* (survival factors), *TNF-α* (a cytokine and positive feedback factor), and *Ptsg2/COX2* (an inflammation modulator), all direct targets of RelA,[21] were all markedly upregulated in the F/F pancreas (Figure 2D and Table 1B, 30 days). It is potentially noteworthy that genes encoding cytokines, including *IL-6*, *IL-1β* and *Ccl2*, which are transcriptionally regulated by the TNF pathway,[23] also showed an

upward trend in expression in the F/F pancreas (Table 1C, 30 days) but that increase was not significant.

In summary, in the pancreas of cKP mice, *Ppp6c* deficiency activated Erk and RelA within 30 days and upregulated genes functioning in proliferation, cell survival, and inflammation. Moreover, Erk and RelA activation occurred at precancerous lesions, suggesting that activation functions in carcinogenesis.

3.3 | Ppp6c loss promotes development and malignant transformation of pancreatic ductal adenocarcinoma in cKP mice

To determine how *Ppp6c* deficiency impacts tumorigenesis, we performed experiments with cKP(+/+) (n = 7), cKP(F/+) (n = 6), and cKP(F/F) (n = 6) mice using the system shown in Figure 1B and analyzed the pathological features of pancreas in 80 day-old mice. cKP(F/F) mice showed significant weight loss (~20%) compared with

TABLE 1 Ratio of gene expression in F/F to F/+ pancreas at 30 and 80 days of age

Genes	30 days		80 days	
	logFC	q-value	logFC	q-value
A ERK signaling pathway				
ELK targets				
FOS	1.67	0.0003	4.99	0.0003
EGR-1	1.69	0.0003	3.14	0.0003
Negative feedback regulators				
DUSP4	4.16	0.0003	4.39	0.0003
DUSP5	1.15	0.0040	3.14	0.0003
DUSP6	1.22	0.0003	3.06	0.0003
DUSP10	3.37	0.0003	2.74	0.0006
B NFκB signaling pathway				
Survival				
Bcl2a1a/Bcl2-related protein A1a	5.27	0.0003	2.52	0.0220
Bcl2a1b/Bcl2-related protein A1b	4.37	0.0003	3.48	0.0003
Positive feedback (inflammation)				
Tnf/TNF-α	3.73	0.0070	3.28	0.0612
Synthesis of inflammatory mediators				
Ptgs2/COX2	2.84	0.0003	4.61	0.3370
C TNF signaling pathway (cytokines)				
IL-6	3.89	0.1250	10.00	0.0003
IL-1	3.26	0.2970	5.60	0.3639
Ccl2/MIC-1	2.45	0.0003	3.84	0.0028
D EMT related				
N-Cadherin	2.16	0.0003	4.02	0.0003
E-Cadherin	0.64	0.0020	−1.72	0.0010
vimentin	1.01	0.0003	3.23	0.0003
Snail	2.12	0.0050	3.45	0.0003
Slug	−0.21	0.7120	2.70	0.0180
ZEB1	0.43	0.0057	1.73	0.0003
E Metabolism related				
Glucose transporter type 1 (Glut1)	0.67	0.0040	1.90	0.0003
Hexokinase 1 (HK1)	0.43	0.0720	2.03	0.0003
Hexokinase 2 (HK2)	−0.21	0.3970	1.18	0.0061
Glucose 6-phosphate dehydrogenase (G6PD)	0.49	0.0280	0.88	0.1520
6-phosphogluconate dehydrogenase (PDG)	2.42	0.0003	1.09	0.0110
Phosphoglucose isomerase (GPI)	0.04	0.8780	0.09	0.8462

TABLE 1 (Continued)

Genes	30 days		80 days	
	logFC	q-value	logFC	q-value
Phosphofructo kinase (PFKL)	0.52	0.0200	1.12	0.0018
Phosphofructo kinase (PFKP)	0.90	0.0530	2.30	0.0058
Aldolase A (ALDOA)	−0.09	0.7500	0.32	0.4846
Aldolase C (ALDOC)	0.21	0.6020	0.18	0.8260
Glyceraldehyde 3-phosphate Dehydrogenase (GAPDH)	0.52	0.0180	1.21	0.0180
Phosphoglycerate kinase 1 (PGK1)	0.75	0.1480	0.75	0.0620
Enolase 1 (ENO1)	0.04	0.8780	1.99	0.0003
Pyruvate kinase 2 (PKM2)	0.36	0.0640	1.29	0.0090
Lactate dehydrogenase a (LDHa)	0.94	0.0003	1.29	0.0020
Lactate dehydrogenase b (LDHb)	0.12	0.8180	0.89	0.1347
F Pancreatic secretion				
Amylase alpha 1	−1.43	0.0003	−4.98	0.0003
Amylase alpha 2B	−2.42	0.0003	−10.00	0.0110
Pancreatic lipase	−2.02	0.0150	−10.00	0.0003
Pancreatic lipase-related protein 1	−1.40	0.0290	−10.00	0.0180
Carboxyl ester lipase	−2.12	0.0100	−10.00	0.0003
Serine protease 1	0.93	0.0003	−7.42	0.0010
Carboxypeptidase B1	−1.76	0.0320	−10.00	0.0003
Chymotrypsin-like	−1.96	0.0010	−10.00	0.0003
Trypsin 4	−2.14	0.0003	−10.00	0.0003

cKP(+/+) or (F/+) mice at this time point (Figure 3A). We then performed pathological analysis of foci of ADM and low- and high-grade intraepithelial neoplasia (LG-PanIN and HG-PanIN) in H&E-stained sections (Figure 3B): cKP(F/F) mice exhibited significantly increased numbers of precancerous lesions compared with +/+ and F/+ genotypes (Figure 3B), and all six F/F mice developed pancreatic tumors (Figure 3C). By contrast, tumors were seen in one out of seven mice of +/+ genotype and in two out of six mice with the F/+ genotype (Figure 3C). Tumors seen in +/+ and F/+ genotypes were pathologically diagnosed as well differentiated PDAC, while F/F genotypes were analyzed as moderately to poorly differentiated PDAC by three independent pathologists. Tumor diameters were larger in F/F relative to F/+ and +/+ genotypes (Figure 3C). Of the six tumors seen in F/F genotype mice, two showed duodenum invasion and one showed lymph node invasion (data not shown). As shown in Figure 3D,a representative tumor in pancreas of F/F mice was classified as moderately
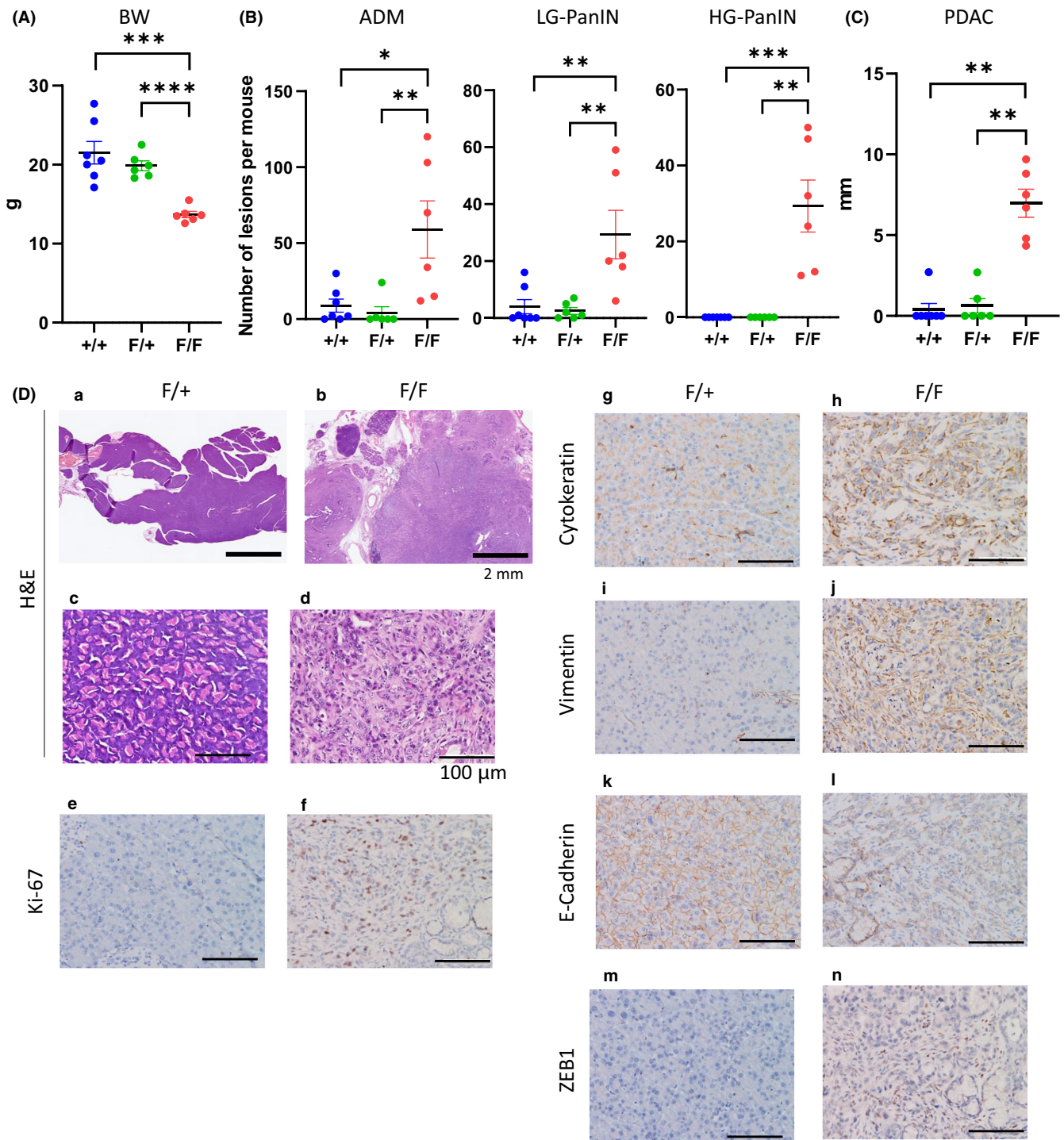
FIGURE 3 Ppp6c deletion promotes weight loss and pancreatic tumor development in cKP mice at 80 days of age. cKP(+/+) (*n* = 7), cKP(F/+) (*n* = 6), and cKP(F/ F) (*n* = 6) mice were administered TAM as described in Figure 1B, and the pancreas was analyzed at 80 days of age. (A) Body weight (BW) of mice of indicated genotypes. (B) Number of foci of ADM, LG-PanIN, and HG-PanIN in mice of indicated genotypes. The *Y*-axis indicates the number of lesions per mouse. (C) PDAC size in mice of indicated genotype. *Y*-axis indicates diameter of the largest tumor developed in one mouse. (D) Representative pancreas of cKP(F/+) (left) and cKP(F/F) (right) mice. H&E staining at low (a, b) and high (c, d) magnification, and IHC using anti-Ki67 (e, f), anti-cytokeratin (g, h), anti-vimentin (i, j), anti-E-cadherin (k, l), and anti-ZEB1 (m, n) antibodies. Scale bar: 2 mm (low magnification) or 100 μm (high magnification)

to poorly differentiated PDAC (Figure 3Db,d). Tumor cell nuclei differed in size and showed pleomorphism (Figure 3Dd) and were Ki67 positive, indicative of renewed proliferation (Figure 3Df). Tumor cells were cytokeratin positive and surrounded by vimentin-positive atypical stromal cells (Figure 3Dh,j). We also observed decreased E-cadherin expression in some regions of the tumor (Figure 3Dl), and

identified ZEB1, a key transcription factor that induces the EMT, in the nucleus of some cancer cells (Figure 3Dn). These findings suggested the occurrence of the EMT.[24]

3.4 | Pancreatic tumors in F/F mice at 80 days show upregulated cytokine production, EMT induction and increased glycolysis marked by high lactate production

We next compared gene expression in pancreatic tissue of F/F versus F/+ genotypes and found that patterns at 80 days differed greatly (Figure 4A). As shown in Table 1, upregulation of Erk (Table 1A), NFκB (Table 1B), and TNF (Table 1C) transcripts in F/F genotype mice seen at 30 days persisted until day 80. Similarly, levels of four inflammatory cytokines, including TNF-α, IL-1β and Ccl2, and IL-6 in particular, were elevated in the sera of F/F compared with F/+ and +/+ mice (Figure 4B). By contrast, serum albumin was relatively low in F/F mice at 80 days, indicating low nutritional status (Figure 4C).

Regarding EMT-related genes, we observed the upregulation of *cytokeratin7,19 and 20* (epithelial cell markers), *vimentin* (a mesenchymal cell marker) and *Snail* and *ZEB1* (EMT transcriptional activators) expression in F/F mice (Table 1D, 80 days), indicating enhanced proliferation of tumor and stromal cells in F/F relative to F/+ pancreas. Higher expression of *Snail* and *ZEB1* in F/F versus F/+ tissues was more pronounced at day 80 compared with at day 30, and these patterns may mark the onset of the EMT.

As for metabolism-related genes, expression of *Glut1* (a glucose transporter) and rate-limiting glycolytic enzymes[25] (*HK1, HK2, PFKL,* and *PFKP*) increased in F/F relative to F/+ pancreas (Table 1E; 80 days), as did expression of *LDHa* and *LDHb*, which function in lactate synthesis (Table 1E; 80 days), suggesting enhanced glycolysis with flux to lactate. Therefore we performed metabolomic analysis to determine the significance of increased expression of glycolytic enzymes. Metabolites found in the pancreas of F/F genotype samples shown in Figure 3 were compared with those observed in F/+ genotype mice. Metabolite expression in F/F and F/+ pancreatic tissues is shown in a heatmap (Figure 4D).

Increases in lactate (5.4-fold) seen in the F/F relative to F/+ pancreas were statistically significant ($p = 0.023$) (Figure 4E). These findings, coupled with elevated expression of glycolytic enzymes, suggested the presence of the Warburg effect in PDAC arising in the F/F pancreas.[26]

In addition, the expression of 6-phosphogluconate dehydrogenase (PDG), which acts in the pentose phosphate pathway, was found to be upregulated in F/F (Table 1E; 80 days). This finding suggested that nucleic acid synthesis is promoted in F/F relative to F/+ pancreas.

3.5 | Ppp6c deficiency promotes skeletal muscle wasting and loss of adipose tissue in cKP mice

Recent analysis showed human PDAC cell-derived IL-6 induces muscle atrophy and adipocyte lipolysis in mice.[27] As levels of circulating IL-6 in F/F type mice are significantly higher than in F/+ mice (Figure 4B), we compared muscle and fat in each genotype, as shown in Figure 5. Figure 5A shows representative gastrocnemius muscle of mice of the three different genotypes (top row). Transverse sections of muscle tissue shown in lower panels (Figure 5A) revealed thinner muscle and smaller myofibrils in F/F mice (Figure 5B).

IL-6 signaling reportedly upregulates transcription of genes encoding E3 ligases (*Atrogin1* and *MuRF1*)[28] and autophagy-related proteins (*Atg5* and *Bnip3*)[28] in muscle, causing muscle atrophy in cachexia.[28] Expression of all four of these genes was markedly upregulated in the F/F gastrocnemius muscle (Figure 5C). Next, we examined the effects on adipose tissue in four male mice from each of the three genotypes. Weight of epididymal adipose tissue in F/F mice was markedly reduced compared with F/+ and +/+ genotypes (Figure 5D). We also observed decreased levels of free fatty acids and glycerol, both of which resulted from adipose tissue breakdown,[29] in sera of F/F type mice, suggesting significant depletion of adipose tissue in F/F genotype mice by 80 days of age (Figure 5D). A hypotrophic state may also be due to pancreatic dysfunction. Relevant to this possibility, at the 80-day time point, we confirmed that levels of amylases (amylase alpha1 and 2B), lipases (pancreatic lipase, pancreatic lipase-related protein 1, carboxy ester lipase), and proteinases (serine protease 1, carboxypeptidase B1, chymotrypsin-like, and trypsin 4) were dramatically reduced in pancreas of F/F compared with F/+ mice (Table 1F; 80 days).

4 | DISCUSSION

Here, we report that *Ppp6c* loss in the pancreas of cKP mice promotes death from cancer within 150 days of induction of the

---

FIGURE 4 Ppp6c deletion increases glycolytic metabolism and expression of cytokine genes in cKP pancreatic tissue by 80 days of age. Pancreatic samples and sera collected at time of sacrifice in the experiment shown in Figure 3 are analyzed in this figure. (A) Heatmap analysis of gene expression in pancreas of cKP(F/F) and cKP(F/+) mice. Among samples shown in Figure 3, three F/F and three F/+ type were used for transcriptome analysis. In total, 19,729 genes expressed in at least one group in each comparison were used for analysis. Red and green colors indicate high and low expression levels, respectively. (B) Elevated levels of cytokines in sera of cKP(F/F) mice. Sera were derived from mice shown in Figure 3. Serum levels of indicated factors were measured. Statistical analysis was carried out using the Mann–Whitney *U* test. (C) Decreased albumin levels in sera of cKP(F/F) mice. Sera evaluated and statistical methods are the same as those in (B). (D) Heatmap analysis of metabolites in pancreas of cKP(F/F) and cKP(F/+) mice. Six samples of F/F type and five of the F/+ type were used for metabolomic analysis. Columns represent individual mice, and rows represent specific metabolites. (E) Glycolysis pathway. Data shown in (D) were used for this analysis. Y-axes show detected average value with standard deviation (error bars) for each comparison: F/F (red) and F/+ (blue). Data are presented as means ± standard deviation from six (for F/F) and five (for F/+) mice
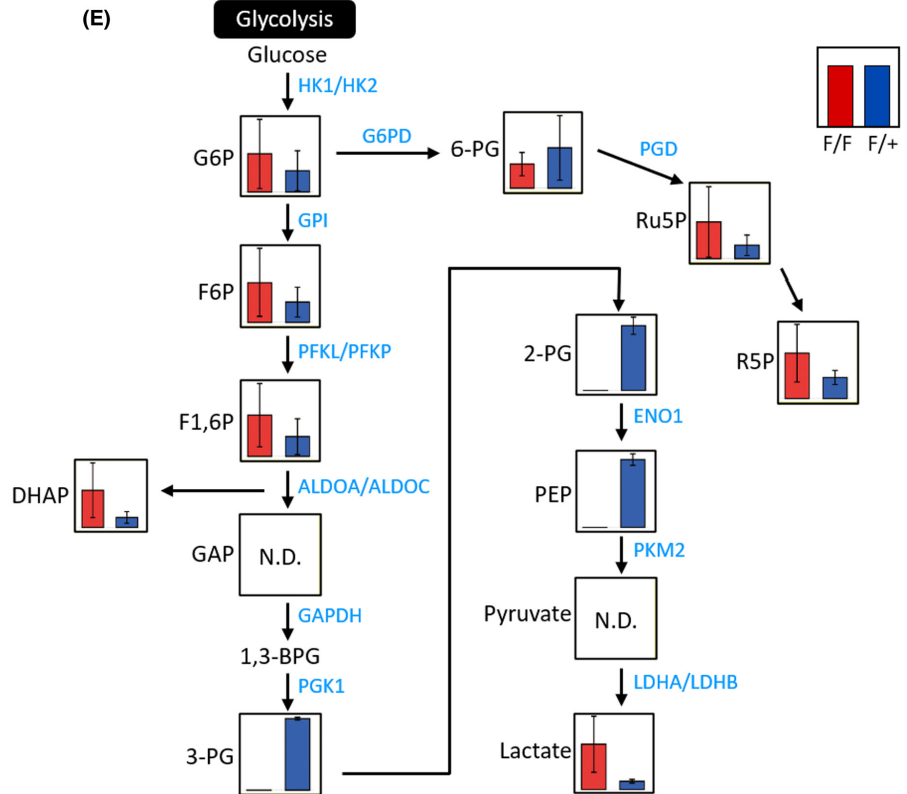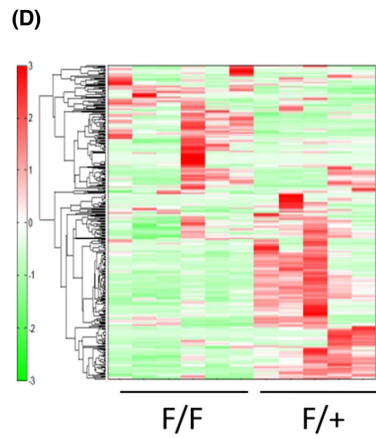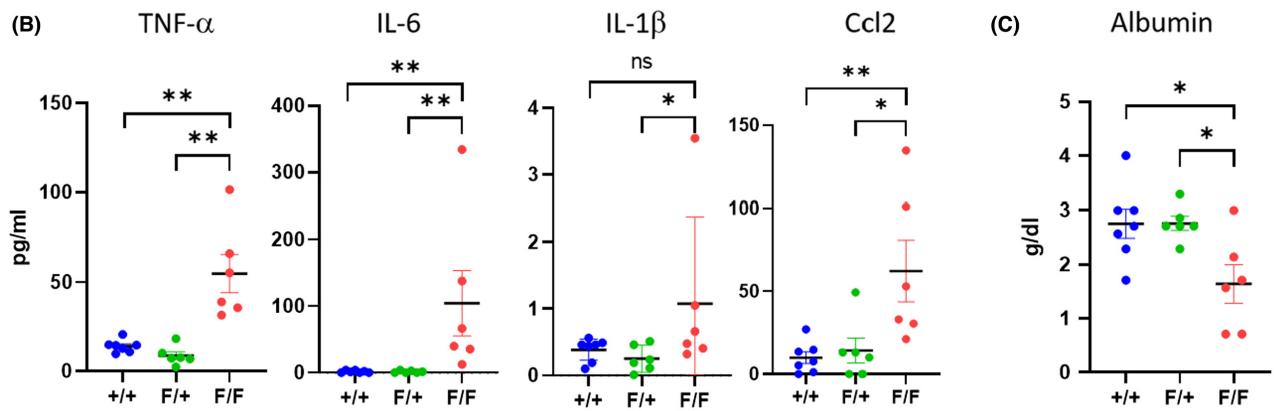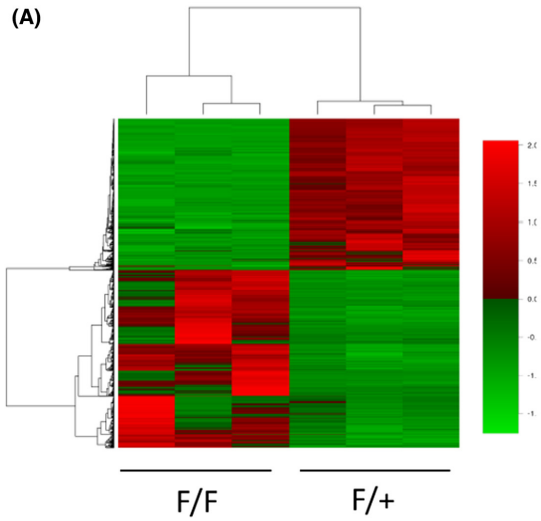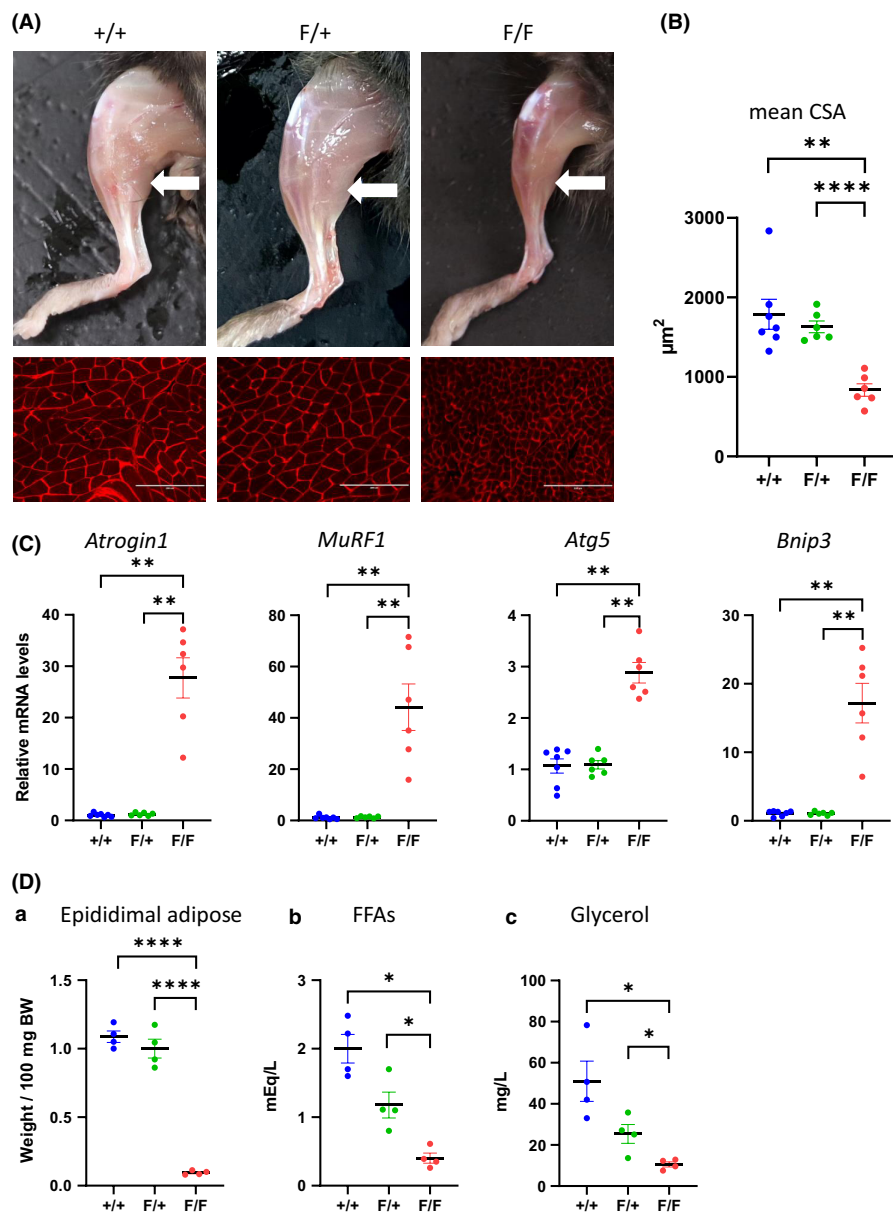
FIGURE 5 Ppp6c loss in pancreas of cKP mice promotes muscle atrophy and loss of adipose tissue at 80 days of age. Tissues and sera used here were derived from animals obtained described in Figure 3. (A) Gross (upper) and cross-sectional (lower) views of gastrocnemius muscle 80 days after TAM administration. Arrows indicate representative gastrocnemius from each indicated genotype. Sections of muscle were stained with laminin antibody. Scale bar: 200 μm. (B) Cross-sectional area (CSA) of gastrocnemius muscles of indicated genotypes. Statistical analysis was carried out using Student's *t* test. (C) *Atrogin1*, *MuRF1*, *Atg5*, and *Bnip3* expression in gastrocnemius muscle of indicated mice. Results were normalized to 18S ribosomal RNA and shown as fold differences in transcript level relative to that seen in the cKP(+/+) pancreas, a value set to 1. Values represent the mean ± SE. Statistical analysis was carried using Student's *t* test. (D) Amount of epididymal adipose tissue and concentrations of serum free fatty acids (FFAs) and serum glycerol in mice of indicated genotypes. Statistical analysis for adipose tissue was carried out using the Mann–Whitney *U* test, and for FFA and glycerol using Student's *t* test

mutation. When compared with *Ppp6c* hemizygous or wild-type cKP mice at 80 days after induction, *Ppp6c*-deficient mice showed accelerated cancer development and progression, and wasting with cachexia. We conclude that *Ppp6c* is a novel pancreatic tumor suppressor gene. To the best of our knowledge, ours is the first demonstration that a serine/threonine phosphatase functions as a tumor suppressor gene in mouse pancreatic carcinogenesis.

Transcriptome analysis of the pancreas at 30 days after mutagenesis showed that the double mutation (KRAS(G12D) expression + loss of Trp53) combined with homozygous *Ppp6c* deletion significantly activated the Erk and NFκB pathways. Erk activation is likely to increase proliferation through fos activation,[22] while NFκB activation may promote cell survival (by Bcl2a1a and Bcl2a1b)[21] and induce inflammation by COX2 secretion[30] and activation of proinflammatory cytokines, including IL-6, IL-1β, Ccl2, and TNF-α, in a positive feedback manner (via TNF-α secretion).[23] Importantly, Erk

and RelA activation occurred mainly in ADM, suggesting that these activities trigger carcinogenesis.

In the pancreas of *Ppp6c* homozygous-deficient cKP mice at 80 days after mutation induction, *Snail* and *ZEB1*[24] expression was upregulated, and pathologically EMT development was confirmed. In addition, Warburg effect-like metabolic changes such as increased glycolysis and lactate production[26] occurred, and invasion of organs by tumor cells was observed in half of the F/F mice. Therefore, *Ppp6c* deficiency in cKP pancreas is likely to promote malignancy.

Phenotypes seen in cKP(F/F) mice at the 80 day time point included weight loss, low serum albumin, muscle atrophy, loss of adipose tissue, and increased levels of inflammatory cytokines in serum, which is indicative of cachexia.[31–33] High serum IL-6 levels also are likely to account for reduction in muscle and adipose tissue in these mice, as has been reported.[27] cKP(F/F) mice exhibited

symptoms of cachexia similar to those seen in human pancreatic cancer.[32,33] Here 85% of pancreatic cancer patients exhibit cachexia, which causes 30% of pancreatic cancer deaths,[33] and treatments for this condition are urgently needed.[34] Our findings indicated that cKP(F/F) mice are a good model for developing treatments for this condition.

Although *Ppp6c* mutations (<1%) or loss of heterozygosity (LOH) have rarely been observed in pancreatic cancer tissues in the COSMIC database,[35] TCGA database shows that prognosis of pancreatic cancer patients whose tumors show low *Ppp6c* mRNA expression is worse than that of patients with high expression (Figure S1). In humans, decreased levels of *Ppp6c* mRNA or PP6 protein may underlie the development of pancreatic cancer. Previous reports have indicated that *Ppp6c* mRNA expression is decreased by *miR-373* in hepatocarcinoma.[36] It was also recently reported that PP6 protein is regulated by p62-dependent autophagy in HeLa cells, and PP6 protein and p62 protein levels are positively correlated in tumor tissues.[37] In particular, in pancreatic cancer, autophagy has been shown to positively regulate tumor growth.[38] Therefore it remains necessary to analyze how changes in PP6 protein function in carcinogenesis locally in the pancreas.

The present study suggests that PP6 inhibits tumorigenesis and malignant transformation by blocking overactivation of Erk and NFκB pathways in pancreatic cells with KRAS mutation and Trp53 deficiency. Therefore, combining MEK/Erk inhibitors with NFκB inhibitors may be effective in treating pancreatic tumors with these mutations. Conversely, as targeted anti-cancer therapy, approaches to activate phosphatases with tumor suppressor activity have been proposed,[39] and small molecule activators of PP2A, which belongs to the same subgroup as PP6, have been developed and shown to be effective in several mouse carcinogenesis models.[40] Activators of PP6 are expected to be developed and could lead to novel therapies.

DISCLOSURE

The authors declare no conflict of interest. N. Tanuma and H. Shima are Editorial Board Members of Cancer Science. All authors had full access to all of the data in the study and had final responsibility for the decision to submit for publication.

ORCID

Nobuhiro Tanuma https://orcid.org/0000-0001-7914-1380
Keiichi Tamai https://orcid.org/0000-0003-0813-5885
Toru Furukawa https://orcid.org/0000-0002-1083-2324
Hiroshi Shima https://orcid.org/0000-0002-0857-8929

REFERENCES

1. Siegel RL, Miller KD, Fuchs HE, et al. Cancer statistics, 2021. *CA Cancer J Clin*. 2021;71(1):7-33.
2. Makohon-Moore A, Iacobuzio-Donahue CA. Pancreatic cancer biology and genetics from an evolutionary perspective. *Nat Rev Cancer*. 2016;16(9):553-565.
3. The Cancer Genome Atlas Research Network. Integrated genomic characterization of pancreatic ductal adenocarcinoma. *Cancer Cell*. 2017;32(2):185-203.
4. Park W, Chawla A, O'Reilly EM. Pancreatic cancer: a review. *JAMA*. 2021;326(9):851-862.
5. Moore AR, Rosenberg SC, McCormick F, Malek S. RAS-targeted therapies: is the undruggable drugged? *Nat Rev Drug Discov*. 2020;19(8):533-552.
6. Ma X, Lu J-Y, Dong Y, et al. PP6 disruption synergizes with oncogenic Ras to promote JNK-dependent tumor growth and invasion. *Cell Rep*. 2017;19(13):2657-2664.
7. Kishimoto K, Kanazawa K, Nomura M, et al. *Ppp6c* deficiency accelerates *K-ras^G12D* -induced tongue carcinogenesis. *Cancer Med*. 2021;10(13):4451-4464.
8. Ohama T. The multiple functions of protein phosphatase 6. *Biochim Biophys Acta Mol Cell Res*. 2019;1866(1):74-82.
9. Ziembik MA, Bender TP, Larner JM, Brautigan DL. Functions of protein phosphatase-6 in NF-kappaB signaling and in lymphocytes. *Biochem Soc Trans*. 2017;45(3):693-701.
10. Stefansson B, Brautigan DL. Protein phosphatase 6 subunit with conserved Sit4-associated protein domain targets IκBε. *J Biol Chem*. 2006;281(32):22624-22634.
11. Kajino T, Ren H, Iemura S-I, et al. Protein phosphatase 6 down-regulates TAK1 kinase activation in the IL-1 signaling pathway. *J Biol Chem*. 2006;281(52):39891-39896.
12. Cho E, Lou HJ, Kuruvilla L, et al. PPP6C negatively regulates oncogenic ERK signaling through dephosphorylation of MEK. *Cell Rep*. 2021;34(13):108928.
13. Hodis E, Watson I, Kryukov G, et al. A landscape of driver mutations in melanoma. *Cell*. 2012;150(2):251-263.
14. Bonilla X, Parmentier L, King B, et al. Genomic analysis identifies new drivers and progression pathways in skin basal cell carcinoma. *Nat Genet*. 2016;48(4):398-406.
15. Kanazawa K, Kishimoto K, Nomura M, et al. *Ppp6c* haploinsufficiency accelerates UV-induced BRAF(V600E)-initiated melanomagenesis. *Cancer Sci*. 2021;112(6):2233-2244.
16. Kato H, Kurosawa K, Inoue Y, et al. Loss of protein phosphatase 6 in mouse keratinocytes increases susceptibility to ultraviolet-B-induced carcinogenesis. *Cancer Lett*. 2015;365(2):223-228.
17. Hayashi K, Momoi Y, Tanuma N, et al. Abrogation of protein phosphatase 6 promotes skin carcinogenesis induced by DMBA. *Oncogene*. 2015;34(35):4647-4655.
18. Kudo K, Nomura M, Sakamoto Y, et al. Divergent metabolic responses dictate vulnerability to NAMPT inhibition in ovarian cancer. *FEBS Lett*. 2020;594(9):1379-1388.
19. Kurosawa K, Inoue Y, Kakugawa Y, et al. Loss of protein phosphatase 6 in mouse keratinocytes enhances *K-ras^G12D*-driven tumor promotion. *Cancer Sci*. 2018;109(7):2178-2187.
20. Morita M, Sato T, Nomura M, et al. PKM1 confers metabolic advantages and promotes cell-autonomous tumor cell growth. *Cancer Cell*. 2018;33(3):355-367.
21. DiDonato JA, Mercurio F, Karin M. NF-κB and the link between inflammation and cancer. *Immunol Rev*. 2012;246(1):379-400.
22. Roskoski RJ. Targeting ERK1/2 protein-serine/threonine kinases in human cancers. *Pharmacol Res*. 2019;142:151-168.
23. Caldwell AB, Cheng Z, Vargas JD, et al. Network dynamics determine the autocrine and paracrine signaling functions of TNF. *Genes Dev*. 2014;28(19):2120-2133.

24. Lamouille S, Xu J, Derynck R. Molecular mechanisms of epithelial-mesenchymal transition. *Nat Rev Mol Cell Biol*. 2014;15(3):178-196.

25. Kodama M, Oshikawa K, Shimizu H, et al. A shift in glutamine nitrogen metabolism contributes to the malignant progression of cancer. *Nat Commun*. 2020;11(1):1320.

26. Liberti M, Locasale JW. The Warburg effect: how does it benefit cancer cells? *Trends Biochem Sci*. 2016;41(3):211-218.

27. Rupert JE, Narasimhan A, Jengelley DHA, et al. Tumor-derived IL-6 and trans-signaling among tumor, fat, and muscle mediate pancreatic cancer cachexia. *J Exp Med*. 2021;218(6):e20190450.

28. Sartori R, Romanello V, Sandri M. Mechanisms of muscle atrophy and hypertrophy: implications in health and disease. *Nat Commun*. 2021;12(1):330.

29. Agustsson T, Rydén M, Hoffstedt J, et al. Mechanisms of increased lipolysis in cancer cachexia. *Cancer Res*. 2007;67(11):5531-5537.

30. Hashemi Goradel N, Najafi M, Salehi E, et al. Cyclooxygenase-2 in cancer: a review. *J Cell Physiol*. 2019;234(5):5683-5699.

31. Fearon KC, Glass DJ, Guttridge DC. Cancer cachexia: mediator, signaling, and metabolic pathway. *Cell Metab*. 2012;16(2):153-166.

32. Poulia KA, Sarantis P, Antoniadou D, et al. Pancreatic cancer and cachexia-metabolic mechanisms and novel insights. *Nutrients*. 2020;12(6):1543.

33. Talbert EE, Cuitiño MC, Ladner KJ, et al. Modeling human cancer-induced cachexia. *Cell Rep*. 2019;28(6):1612-1622.e4.

34. Qin C, Yang G, Yang J, et al. Metabolism of pancreatic cancer: paving the way to better anticancer strategies. *Mol Cancer*. 2020;19(1):50.

35. Tate JG, Bamford S, Jubb HC, et al. COSMIC: the Catalogue Of Somatic Mutations In Cancer. *Nucl Acids Res*. 2019;47(D1):D941-947.

36. Wu N, Liu X, Xu X, et al. MicroRNA-373, a new regulator of protein phosphatase 6, functions as an oncogene in hepatocellular carcinoma. *FEBS J*. 2011;278(12):2044-2054.

37. Fujiwara N, Shibutani S, Sakai Y, et al. Autophagy regulates levels of tumor suppressor enzyme protein phosphatase 6. *Cancer Sci*. 2020;111(12):4371-4380.

38. Piffoux M, Eriau E, Cassier PA. Autophagy as a therapeutic target in pancreas cancer. *Br J Cancer*. 2021;124(2):333-344.

39. Westermarck J. Targeted therapies don't work for a reason; the neglected tumor suppressor phosphatase PP2A strikes back. *FEBS J*. 2018;285(22):4139-4145.

40. Leonard D, Huang W, Izadmehr S, et al. Selective PP2A enhancement through biased heterotrimer stabilization. *Cell*. 2020;181(3):688-701.

SUPPORTING INFORMATION

Additional supporting information may be found in the online version of the article at the publisher's website.